Chemosphere xxx (xxxx) 143334

Contents lists available at ScienceDirect

Chemosphere

journal homepage: www.elsevier.com/locate/chemosphere

Removal of aflatoxin M_1 in milk using magnetic laccase/MoS_2/chitosan nanocomposite as an efficient sorbent

Alieh Rezagholizade-shirvan [a], Ahmad Ghasemi [b], Yeganeh Mazaheri [c], Samira Shokri [c], Saeid Fallahizadeh [d, e], Mahmood Alizadeh Sani [f], Mahnaz Mohtashami [g], Maryam Mahmoudzadeh [h], Mansour Sarafraz [i], Majid Darroudi [j], Zeinab Rezaei [k], Ehsan Shamloo [a, *]

[a] Department of Food Science and Technology, Neyshabur University of Medical Sciences, Neyshabur, Iran
[b] Department of Biochemistry, Nutrition and Food Sciences, School of Medicine, Gonabad University of Medical Sciences, Gonabad, Iran
[c] Department of Environmental Health Engineering, Food Safety Division, School of Public Health, Tehran University of Medical Sciences, Tehran, Iran
[d] School of Public Health, Yasuj University of Medical Sciences, Yasuj, Iran
[e] Social Determinants of Health Research Center, Yasuj University of Medical Sciences, Yasuj, Iran
[f] Department of Food Science and Technology, School of Nutritional Sciences and Dietetics, Tehran University of Medical Sciences, Tehran, Iran
[g] Department of Biology, School of Basic Science, Neyshabur Branch, Islamic Azad University, Neyshabur, Iran
[h] Faculty of Nutrition and Food Science, Tabriz University of Medical Sciences, Tabriz, Iran
[i] School of Public Health, Shahroud University of Medical Sciences, Shahroud, Iran
[j] Nuclear Medicine Research Center, Mashhad University of Medical Sciences, Mashhad, Iran
[k] University of Applied Science and Technology, Center of Cheshme noshan khorasan (Alis), Iran

ARTICLE INFO

Keywords:
Molybdenum disulfide
Nanocomposite
Laccase
Aflatoxin M_1
chitosan
Immobilization

ABSTRACT

The current study tries to find the impact of the integration of laccase enzyme (Lac) onto magnetized chitosan (Cs) nanoparticles composed of molybdenum disulfide (MoS_2 NPs) (Fe_3O_4/Cs/MoS_2/Lac NPs) on the removal of AFM_1 in milk samples. The Fe_3O_4/Cs/MoS_2/Lac NPs were characterized by FT-IR, XRD, BET, TEM, FESEM, EDS, PSA, and VSM analysis. The cytotoxic activity of the synthesized nanoparticles in different concentrations was evaluated using the MTT method. The results show that the synthesized nanoparticles don't have cytotoxic activity at concentrations less than 20 mg/l. The ability of the prepared nanoparticles to remove AFM_1 was compared by bare laccase enzyme, MoS_2, and Fe_3O_4/Cs/MoS_2 composite, indicating that the Fe_3O_4/Cs/MoS_2/Lac NPs the highest adsorption efficiency toward AFM_1. Besides, the immobilization efficiency of laccase with a concentration range of 0.5–2.0 was investigated, indicating that the highest activity recovery of 96.8% was obtained using 2 mg/ml laccase loading capacity. The highest removal percentage of AFM_1 (68.5%) in the milk samples was obtained by the Fe_3O_4/Cs/MoS_2/Lac NPs at a contact time of 1 h. As a result, Fe_3O_4/MoS_2/Cs/Lac NPs can potentially be utilized as an effective sorbent with high capacity and selectivity to remove AFM_1 from milk samples.

1. Introduction

Mycotoxins are secondary metabolites of filamentous fungi in the genus Aspergillus that can enter human and animal bodies through contaminated agricultural products or animal products (Mimoune et al., 2016; Abdi-Moghadam et al., 2023a). The occurrence of mycotoxin contamination leads to noteworthy financial loss to the food and feed sectors, while also representing a serious threat to human health (Meneely et al., 2023). Aflatoxins (AFs) are considered to be among the most deleterious mycotoxins, which are generated by *Aspergillus flavus*, *Aspergillus parasiticus*, and other fungi that are frequently observed in the manufacturing and conservation of grain and feed (Alameri et al., 2023; Shokri-Jokari et al., 2016; Shamloo et al., 2012; Shamloo and Jalali, 2015). As a result of their toxicological attributes, specifically their carcinogenic, teratogenic, and mutagenic properties, AFs have the potential to cause harm to both animal and human health (Yang et al., 2020; Rezagholizade-Shirvan et al., 2023a,b).

Aflatoxins M_1 (AFM_1) is a metabolite of aflatoxin B_1, one of the environment's most toxic and prevalent mycotoxins (Deng et al., 2018). AFM_1 is formed when dairy animals consume feed contaminated with

* Corresponding author.
E-mail address: e.shamloo@yahoo.com (E. Shamloo).

https://doi.org/10.1016/j.chemosphere.2024.143334
Received 31 August 2023; Received in revised form 5 September 2024; Accepted 11 September 2024
0045-6535/

aflatoxin B1, which is excreted in their milk, posing a risk to humans who consume dairy products (Min et al., 2021). The toxicological and carcinogenic impacts of AFM_1 have been demonstrated, leading the International Agency for Research on Cancer-World Health Organization (IARC-WHO) to conduct a reassessment of its carcinogenicity classification and upgrade it from group 2 to group 1 (Organization and Cancer, 1993). The maximum limit for milk and infant milk products has been set by the United States at 500 ng/kg and 25 ng/kg respectively, while the European Community (EC) and Codex Alimentarius have stipulated a threshold of 50 ng/kg AFM_1 in milk and 25 ng/kg for infant milk products. Notably, Austria and Switzerland have established an even lower maximum level of 10 ng/kg for infant food commodities (Fallah, 2010; Abdi-Moghadam et al., 2023b).

The consumption of AFM_1-contaminated food and feed can have severe side effects on human health. Chronic exposure to AFM_1 has been linked to an increased risk of liver cancer, particularly in populations with high levels of contamination in their diet (Schrenk et al., 2020). In addition to its carcinogenic properties, AFM_1 can also cause acute toxicity, leading to symptoms such as liver damage, immune suppression, and growth retardation (Pickova et al., 2021). AFM_1 contamination in feed can result in reduced milk production, impaired reproductive performance, and liver damage in animals (Seid and Mama, 2019).

Given the serious health risks associated with AFM_1, it is crucial to implement measures to remove this toxin from food and feed supplies. Adsorption procedures have been widely studied and employed for removing aflatoxins from contaminated samples (Muaz et al., 2024; Hamad et al., 2023). Adsorption is a process that involves the binding of aflatoxin molecules to a solid surface as a sorbent (Ghorbani et al., 2020a,b 2024). These sorbents have high surface areas and specific binding sites that can effectively capture aflatoxin molecules from the surrounding environment (Gordi et al., 2020).

The importance of removing AFM_1 through adsorption procedures cannot be overstated. By effectively reducing the levels of AFM_1 in food and feed, the risk of exposure to this toxic compound can be minimized, thereby protecting the health of humans and animals. Adsorption-based methods offer a cost-effective and efficient means of removing AFM_1 from contaminated samples, making them a valuable tool in food safety and animal health practices (Ghorbani et al., 2017).

Sorbents play a crucial role in the adsorptive removal of AFM_1 from food and feed products (Aoyanagi et al., 2023; Jahanmard et al., 2021). Sorbents are materials that have the ability to selectively bind and remove contaminants like AFM_1 from a solution through the process of adsorption, leading to high adsorption capacities and selectivity toward AFM_1 (Ghorbani et al., 2019, 2020a,b). Therefore, preparing a new and efficient sorbent is important for removing AFM_1 while leaving other compounds in the solution unaffected. This ensures that the adsorptive removal process is efficient and does not lead to the loss of valuable nutrients or compounds present in the food or feed (Othman et al., 2018).

Laccase is an enzymatic catalyst that comprises four copper ions and can be obtained from certain microorganisms, such as white rot fungi (Liu et al., 2020). Laccase immobilization employing MoS_2 nanoparticles has been investigated in several researches (Zhang et al., 2020a; Rubio-Govea et al., 2020). The immobilized laccase demonstrated significant loading capacity and activity retention along with high stability across a broad spectrum of pH, temperature, and storage periods. Additionally, it manifested excellent recyclability and adeptness in the removal of cancer-causing pollutants (Muthuvelu et al., 2020). MoS_2 nanoparticles have been found to possess numerous benefits in the context of immobilizing laccase. One of the advantages of utilizing these nanoparticles is the enhancement of enzyme stability and reusability, thereby enabling the occurrence of multiple adsorption-desorption cycles (Alvarado-Ramírez et al., 2021). Furthermore, the immobilized laccase exhibits a substantial percentage of its preliminary activity even after undergoing multiple cycles (Datta et al., 2021). Another benefit that can be attributed to these nanoparticles is their ease of recovery from the reaction mixture through using a magnetic field (Yadav et al., 2021).

In this current investigation, the primary objective is to stabilize the laccase enzyme derived from fungi onto biocompatible and non-toxic nanoparticle support to eliminate aflatoxin from milk. On the other hand, immobilizing laccase on nanoparticles led to the reduction of aflatoxin concentration in milk. For this purpose, a new sorbent (Fe_3O_4/Cs/MoS_2/Lac NPs), including four components (Fe_3O_4, chitosan, MoS_2 NPs, and laccase enzyme), was prepared to remove AFM_1 from milk samples. In the sorbent, MoS_2 NPs with a high surface area was selected as the sorbent core in which the other components place on it. The magnetic Fe_3O_4 NPs were used as a sorbent component to its simple separation from the milk samples after adsorbing AFM_1 on the sorbent surface. Finally, chitosan with amine functional groups and laccase enzyme with carboxyl and amine functional groups were used in the sorbent composite to interact with functional groups of AFM_1 through forming the hydrogen bonds.

2. Method and materials

2.1. Materials

Laccase from Trametes versicolor (specific activity = 136 U/mg), chitosan (low molecular weight, DDA 80%), Trypan blue, foetal bovine serum (FBS), penicillin/streptomycin (Penstrep) and dimethylsulphoxide (DMSO) were purchased from Sigma–Aldrich (St.Louis, MO, USA). Sodium dodecyl benzene sulfonate (NaDBS), Ferric chloride hexahydrate ($FeCl_3{\cdot}6H_2O$), ferrous chloride tetrahydrate ($FeCl_2{\cdot}4H_2O$), Hydrochloric acid (37%), ammonium hydroxide (99%), glacial acetic acid (98%), chloroacetic acid sodium molybdate dehydrate, sodium triphenylphosphine (TPP), glutaraldehyde (50% solution in water) and Bradford reagent were obtained from Merck (Darmstadt, Germany). All reagents utilized were of high purity. All solutions were provided in double distilled water.

2.2. Preparation of Fe_3O_4 NPs

The mixing of 80 mL of deionized water was carried out in a three-necked flask, which underwent a 30-min process of nitrogen purging at a temperature of 65 °C, alongside incessant stirring. After adding $FeCl_3{\cdot}6H_2O$ (2.4 g) and $FeCl_2{\cdot}4H_2O$ (0.9 g), then the pH of the solution was regulated to 9–10 with $NH_3{\cdot}H_2O$ while being stirred for 1 h at 70 °C. The resulting product was isolated utilizing a magnetic bar, and the Fe_3O_4 NPs were washed thoroughly with deionized water and methanol until the pH reached approximately 7. Subsequently, the Fe_3O_4 nanoparticles were subjected to vacuum freeze-drying until a constant weight was achieved (Liang et al., 2019; Farhadi et al., 2022; Khosravi-Darani et al., 2019; Shamloo et al., 2023; Ghorbani et al., 2016).

2.3. Synthesis of Fe_3O_4/Cs/MoS_2 NPs

The procedure for synthesizing Cs/MoS_2 hybrid NPs involves a two-step process. First of all, a solution of chitosan (50 mg or 0.2% W/V) was dissolved in 1% of a 50 mL acetic acid solution under magnetic stirring at 25 °C. Subsequently, MoS_2 nanosheets (25 mg or 0.1% W/V), prepared according to a previous study (Nazifi et al., 2021), were added to the aforementioned chitosan solution. The resulting mixture underwent ultra-sonication for 5 h to create a MoS_2-dispersed chitosan matrix (0.1:0.2% W/V ratio), where the sonication process effectively exfoliated MoS_2 particles into nanosheets. The product was then centrifuged at 6000 rpm for 15 min to isolate any remaining bulk non-exfoliated MoS_2 particles from the reaction mixture. In the second step, a solution containing 20 mg of previously prepared Fe_3O_4 nanoparticles was added to the viscous solution, which was then stirred mechanically

for 2 h at 25 °C. Paraffin, a hydrocarbon mixture consisting of alkane molecules, was added to the dispersion in a quantity of 10 mL, along with the addition of 4 mL of Span-80 emulsifier, a nonionic surfactant, at a temperature of 40 °C through 1 h. Subsequently, a solution of glutaraldehyde (5 mL; 2.5%; v/v), a cross-linking agent commonly used in biological applications, was gradually incorporated into the reaction mixture. To enhance the composite's properties, 25 ml of TPP solution, which is a compound frequently used as a reducing agent, was added and then subjected to ultrasonic treatment for 40 min at room temperature. The modified cross-linking composite was then exposed to heat at 50 °C for 1 h. To obtain the magnetics/MoS_2 NPs, the final product was collected via the application of a magnetic field and subsequently washed twice with ethanol and deionized water. The reaction mixture was then dried in an oven (80 °C) (Farhadi et al., 2022; Khosravi-Darani et al., 2019; Nazifi et al., 2021; Rezagholizade-shirvan et al., 2022; Rezagholizade-shirvan et al., 2023a,b;Rezagholizade-Shirvan et al., 2024; Shokri et al., 2023; Shokri et al., 2024).

2.4. Immobilization of laccase on $Cs/MoS_2/Fe_3O_4$ NPs

First, an amount of 0.1 g of Fe_3O_4/Cs/MoS_2 NPs was added to a solution of Glutaraldehyde (2.5%v/v) and allowed to be treated for 2 h at a temperature of 25 °C. Subsequently, the activated nanocomposite was separated using a magnet and then washed with sodium acetate buffer three times. Secondly, the activated Fe_3O_4/Cs/MoS_2 NPs were poured into a solution of laccase (2 mg/ml) and shaken for 6 h at 25 °C. Ultimately, the immobilized laccase on Fe_3O_4/Cs/MoS_2 NPs (IM-laccase) was isolated, washed repeatedly, and kept in a buffer solution at a temperature of 4 °C (Zhang et al., 2020b; Atabati et al., 2020).

2.5. Characterization of nanocomposite

2.5.1. Interactions

The Fourier infrared spectrometer (FTIR) was attained on Bruker Vector-22 FTIR to determine molecular interactions in the nanocomposite compounds. The FTIR spectra of the prepared KBr tablet containing sorbent were recorded in the number wave range of 500–4000 nm.

2.5.2. Particle size and dispersibility of composite NPs

Transmission Electron Microscopy (TEM, JOEL JEM-3010) was employed to observe the particle size and dispersibility of composite nanoparticles.

2.5.3. Crystallinity of nanoparticles

X-ray diffractometer (XRD) pattern was acquired on a Rigaku-12 KW X-ray diffractometer in the 2 Theta range of 10-80° to investigate crystallinity of nanoparticles.

2.5.4. Magnetic property of nanoparticles

The magnetic feature of NPs was detected through a vibrating sample magnetometer (VSM, Lakeshore).

2.5.5. Morphology of NPs

Field Emission-Scanning Electron Microscopy (MIRA3 TESCAN, Czech Republic) was utilized to study the morphology of the sorbent.

2.5.6. Absorbance property of sorbent

Additionally, the absorbance was determined with an ultraviolet spectrophotometer (UV–Vis, JENWAY 7313, UK).

2.5.7. Analysis of AFM_1

The HPLC Knauer (Germany) equipped with a Eurospher 100/5C18 column was utilized to perform AFM_1 determination. The mobile phase (flow rate of 1.0 ml/min) included phosphate buffer (pH 4, 0.05 mM) and acetonitrile/methanol solution (50:50 v/v) with a ratio of 60:40 v/v. Besides, an emission wavelength of 435 nm and an excitation wavelength of 362 nm were selected for the fluorescence detector (RF-20A fluorescence detector) for determining AFM_1 (Ghorbani et al., 2023).

2.6. Enzymatic activity assay

The enzymatic activity of IM-laccase and bare laccase was assessed using 2,2′-azino-bis(3-ethylbenzothiazoline-6-sulfonic acid) (ABTS) as the substrate.

The enzymatic activity of IM-laccase and bare laccase were assessed by employing 2,2′-azino-bis(3-ethylbenzothiazoline-6-sulfonic acid (ABTS) as the substrate. Specifically, the ABTS solution was prepared using a citrate buffer solution (1 mM) as the substrate. An appropriate quantity of bare laccase or various concentrations (0.5, 1, 1.5, 2 mg/ml) of immobilized laccase were added to the substrate. The mixture was then allowed to react at a fixed temperature for 5 min. Subsequently, the absorbance of the supernatant was measured using a UV–vis spectrometer at 420 nm. The enzymatic activities were evaluated by performing three parallel measurements for each sample and then calculating the average of the results. These measurements were conducted in triplicate to ensure accuracy and reliability. In this assay, one unit (1U) of enzyme activity was defined as the amount of enzyme required to catalyze the oxidation of 1 μmol of substrate per minute. The computation of the activity was determined by following the given formulae:

$$\text{Activity recovery } (\%) = A \times 106 \times V_t \,/\, (\varepsilon \times t \times m)$$

Where A is the absorbance of $ABTS^{2+}$ at $\lambda = 420$ nm; V_t represents the total volume of the volume of the reaction (L); ε is the molar extinction coefficient of ABTS + at $\lambda = 420$ nm (36000 M^{-1} cm^{-1}); t is the reaction time (min); m discusses the total weight of the nanocomposite (g) (Qiu et al., 2021).

2.7. MTT assay

The L929 fibroblast cell line was obtained from the National Cell Bank of Iran (NCBI). The cells were seeded in DMEM medium (Gibco, Germany) supplemented with 10% FBS (Gibco, Germany), 1% penicillin G, and streptomycin, and incubated at 37 °C under 5% CO_2. The effect of conjugated nanoparticles (MoS_2/Fe/Cs and Fe_3O_4/MoS_2/Cs/Lac) and free MoS_2 nanoparticles on cell viability was determined via the MTT assay. Cells (5×10^3 cells/well) were seeded in 96-well plates containing DMEM medium supplemented with 10% FBS and incubated overnight. Cells were then treated with various concentrations (0.0625–160 ppm) of MoS_2, MoS_2/Fe/Cs, or Fe_3O_4/MoS_2/Cs/Lac at 37 °C for 48 h. After treatment, 20 μl MTT reagent (2 mg/ml) was added to each well and incubated at 37 °C for 4 h. Subsequently, 100 μL DMSO was added to each well to solubilize the formazan crystals. The absorbance (OD) of the samples was measured at 570 nm using a Bio-Rad microplate reader (Hercules, California, USA). Cell viability in treated cells was expressed as a percentage of the untreated control.

2.8. Removal of AFM_1 in milk

Several sorbents, including bare laccase, Fe_3O_4/Cs/MoS_2 NPs, and Fe_3O_4/Cs/MoS_2/Lac nanocomposite, were utilized to remove AFM_1 in the spiked milk samples. Each sorbent (40 mg) was individually added to 2 ml milk into microtubes, followed by adding 1 mL of AFM_1 solution (0.5 ppb) to each microtube. The microtubes were then subjected to vortex for 5 min and placed in a shaker-incubator at a temperature of 25 °C for three variety contact times (20, 40, and 60 min). The samples were subsequently isolated from the AFM_1 solution through centrifugation at 29,000 × *g* for 15 min, and the AFM_1 concentration in the supernatant was determined using the HPLC method (Khiavi et al., 2020).

2.9. HPLC method validation

Validation of the HPLC method for determining AFM_1 was conducted for linearity, precision, limit of detection (LOD), and limit of quantification (LOQ). The linearity of this approach was determined by analyzing the responses obtained from injecting three replicates (20 μL) of seven different concentrations of AFM_1 standard solutions (0.1, 0.5, 0.75, 1, 1.25, and 1.5 ng/mL). The calibration curve indicated acceptable linearity (R^2 = 0.999) over the concentration range of 0.02–1.5 ng/mL with a linear equation of Y (Peak area) = 98600C (ng/mL) + 920.9. The method's accuracy was determined through a recovery assay. The recovery of AFM_1 for spiking milk samples with a concentration of 0.5 ng/mL was 98.6%. Precision was evaluated by intra-day and inter-day repeatability experiments. For this purpose, the intra-day and inter-day relative standard deviation was calculated by triplicate determination of AFM1 in the spiked milk samples on one day and three consecutive days, respectively. To prevent AFM_1 degradation, the extracts utilized for inter-day injections were stored under appropriate laboratory conditions at 20 °C in darkness. The intra-day and inter-day RSDs for triplicate determination of AFM_1 with a concentration of 0.5 ng/mL were 1.89 and 2.05%, respectively. Limit of detection (LOD) and limit of quantitation (LOQ) were established for determining AFM_1 through the use of signal-to-noise ratios of 3:1 and 10:1, respectively. The LOD and LOQ for determining AFM_1 were 0.005 and 0.017 ng/mL, respectively.

3. Results and discussion

3.1. Characterization of NPs

3.1.1. TEM analysis

TEM analysis was performed to characterize the structure and morphology of MoS_2, Cs/MoS_2, and Fe_3O_4/Cs/MoS_2/Lac NPs (Fig. 1). TEM images revealed that MoS2 exhibited a thin, smooth, layered structure (Fig. 1a). Cs NPs displayed a homogeneous, porous distribution with spherical morphology, while Cs/MoS_2 displayed a thicker, rough, and less-defined nanostructure. The incorporation of Cs into MoS_2 significantly altered the surface morphology and roughness of the pristine MoS_2 NPs (Fig. 1b and c). Besides, as noted in previous literature, the Fe_3O_4 magnetic nanoparticles with a spherical or elliptical shape and a size lower than 30 nm are displayed on the sorbent surface (Qiu et al., 2021; Khiavi et al., 2020; Kim et al., 2018). In other words, the successful synthesis of Fe_3O_4/Cs/MoS_2/Lac NPs is evidenced by the even distribution of homogenous magnetic nanoparticle particles on the Cs/MoS_2 composite surface.

3.1.2. FE-SEM analysis

The FESEM images of MoS_2 and Fe_3O_4/Cs/MoS_2/Lac NPs are displayed in Fig. 2. In Fig. 2a, it can be observed that the MoS_2 particles exhibit a cylindrical shape with thin threads on their surface. These surface structures enhance the surface area of the compound, leading to improved absorption of AFM_1. Fig. 2b shows the Fe_3O_4/Cs/MoS_2/Lac NPs with significant aggregation, attributed to the magnetic properties of Fe_3O_4 and the polymeric structure of Cs. Additionally, spherical particles can be seen on the surface of the cylindrical MoS_2 particles, likely stemming from the presence of magnetic Fe_3O_4 and Cs nanoparticles. The small size of the Lac particles may explain their absence in this image.

The energy-dispersive X-ray spectroscopy (EDX) pattern of the Fe_3O_4/Cs/MoS_2/Lac nanocomposite is depicted in Fig. 2c. This pattern reveals that the composite material consists of carbon, oxygen, iron, sulfur, nitrogen and molybdian elements, with weight percentages of 16.32%, 47.28%, 35.38%, 0.53%, 0.08% and 0.41%, respectively. Notably, oxygen and nitrogen exhibit the highest and lowest weight percentages within the sorbent structure.

3.1.3. XRD analysis

The XRD test was employed to evaluate the crystalline and amorphous characteristics of the Fe_3O_4/Cs/MoS_2/Lac composite components, as depicted in Fig. 3. The utilization of this technique enabled the determination of the structural properties of the composite, thus providing valuable insights into its composition and morphology. The results obtained from this experiment are crucial in furthering our understanding of the physicochemical properties of the material. Transition metal dichalcogenides, for instance, molybdenum disulfide, have been identified as two-dimensional layered nanostructures, with X-ray diffraction peaks at 2θ = ~15°, ~37.5°, ~44°, and ~66° corresponding to the (002), (100), (103), and (110) crystalline planes of MoS_2 (JCPDS 37–1492) respectively. (Geioushy et al., 2019a; Cao et al., 2019). The introduction of Cs polymer leads to a reduction in the intensity of the XRD peaks of chitosan and MoS_2. This finding provides evidence of a chemical reaction between chitosan and MoS_2 during the process of fabrication, as well as the achievement of great functionalization of the Cs matrix. Moreover, after the incorporation of Fe_3O_4 and Lac into the Cs/MoS_2 composite, the observed peaks, occurring at specific angles of 2θ including 15°, 16.5°, 18°, 30.1°, 32°, 35.2°, 39.8°, 43.2°, 57.2°, and 62.2°, were closely aligned with the distinctive peaks that are typical of the crystal structure of Fe_3O_4 magnetic nanoparticles (JCPDS N° 19–407 0629) (Qiu et al., 2021; Khiavi et al., 2020; Kim et al., 2018; Cao et al., 2019; Geioushy et al., 2019b; Silveira et al., 2020; Yousefi et al., 2024; Azari et al., 2024). The retention of the same characteristic peaks and the unchanged strength of the peaks after the activation of Fe_3O_4/Cs/MoS_2/Lac nanoparticles coated by Cs/MoS_2 composite im-

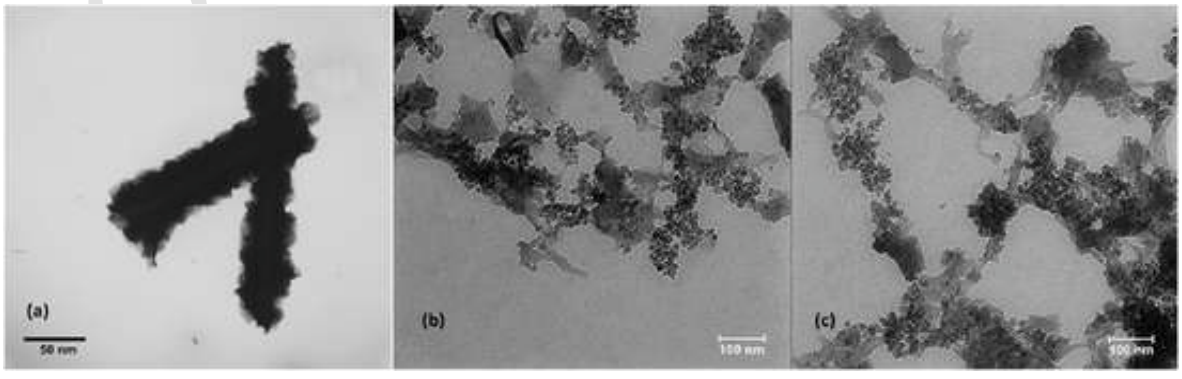

Fig. 1. TEM images of MoS_2 NPs (a) and Fe_3O_4/Cs/MoS_2/Lac NPs (b and c).

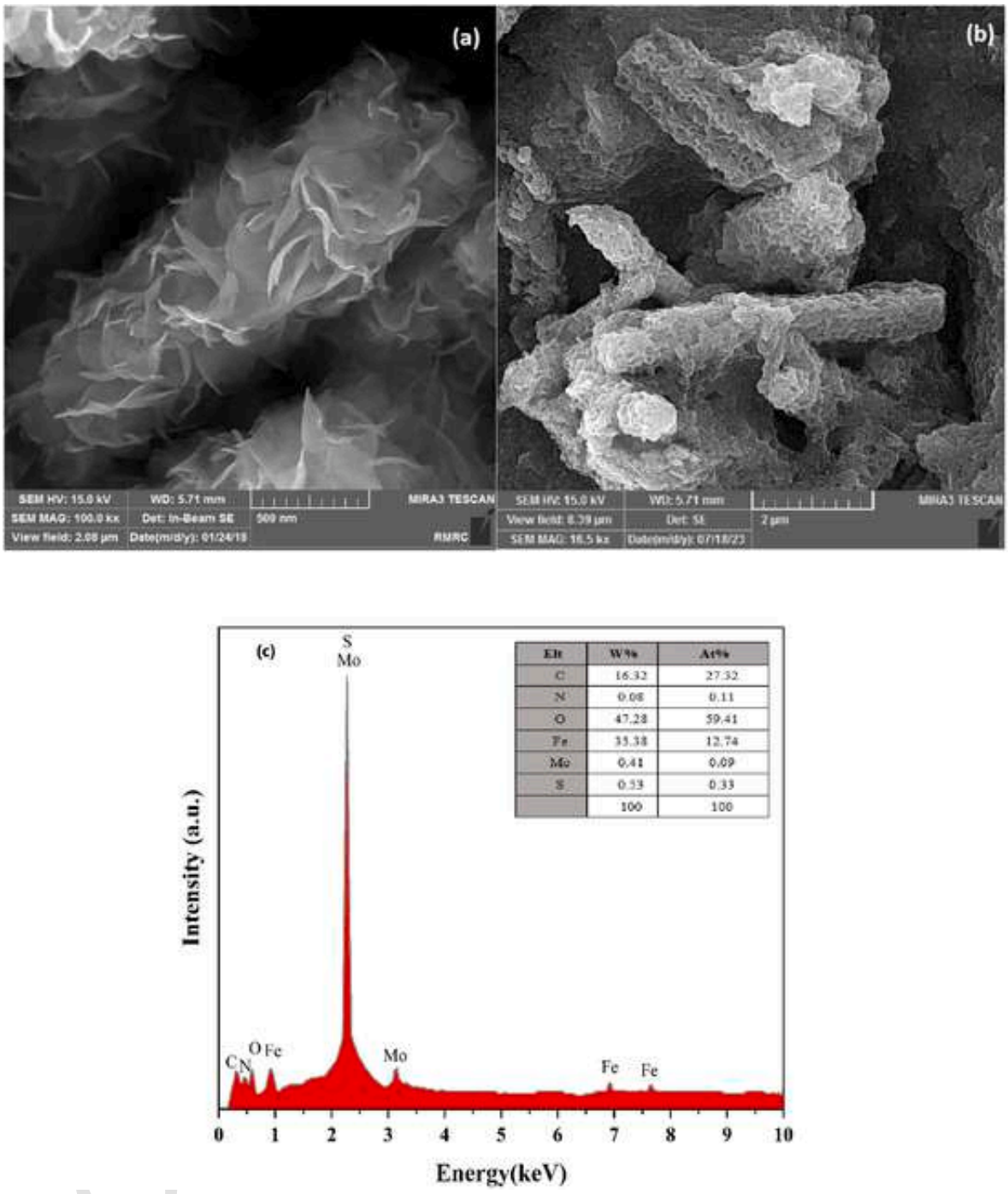

Fig. 2. FESEM images of MoS_2 (a) and Fe_3O_4/Cs/MoS_2/Lac NPs (b), and EDX pattern (c) of the Fe_3O_4/Cs/MoS_2/Lac NPs.

plies ideal compatibility and good interaction with the preservation of the crystal structure of magnetic nanoparticles at a high level.

3.1.4. BET analysis

The porosity of Fe_3O_4/Cs/MoS_2/Lac NPs was examined using BET analysis. The BET plot revealed a BET constant (C) of 69.498, specific surface area (as) of 81.47 $m^2\ g^{-1}$, monolayer adsorption amount (Vm) of 19.06 cm^3 (STP) g^{-1}, adsorption space volumes (Va) of 1497.4, mean pore diameter of 4.5967 nm, and total pore volume of 0.4172 $cm^3\ g^{-1}$. These results suggest that the sorbent possesses an adequate surface area for adsorbing AFM_1. Additionally, the BJH model indicated an ap of 63.194 $m^2\ g^{-1}$, an adsorption pore radius (rp) of 1.32 nm, and a pore volume (PV) of 0.095417 $cm^3\ g^{-1}$. The pore radius of 1.32 nm classifies the prepared composite as a microporous material.

3.1.5. FTIR analysis

FTIR spectroscopy was employed to identify the variety of organic functional groups present in the sorbents. Fig. 4 shows the FTIR spectra of MoS_2, Cs, Lac, Fe_3O_4, MoS_2/Cs/Fe_3O_4, and Fe_3O_4/Cs/MoS_2/Lac NPs. As depicted in Fig. 4, the vibrational spectrum of Cs displays distinctive peaks at various wavenumbers, including 3494 cm^{-1}, 2872 cm^{-1}, 1637 and 1577 cm^{-1}, 1418 cm^{-1}, 1157 cm^{-1}, and 1098 cm^{-1}, which were

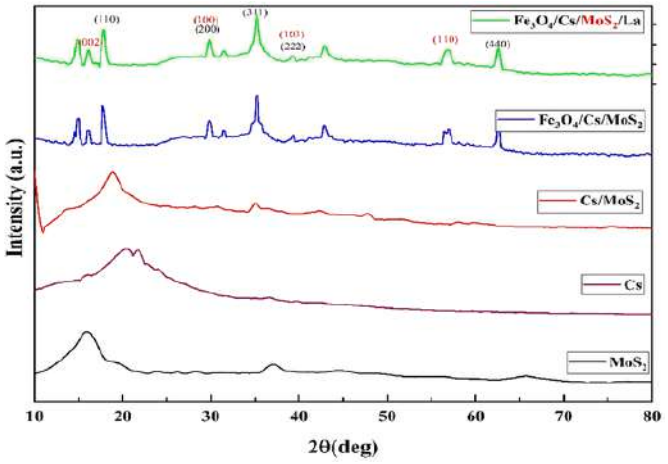

Fig. 3. XRD pattern of Fe_3O_4/Cs/MoS_2/Lac NPs.

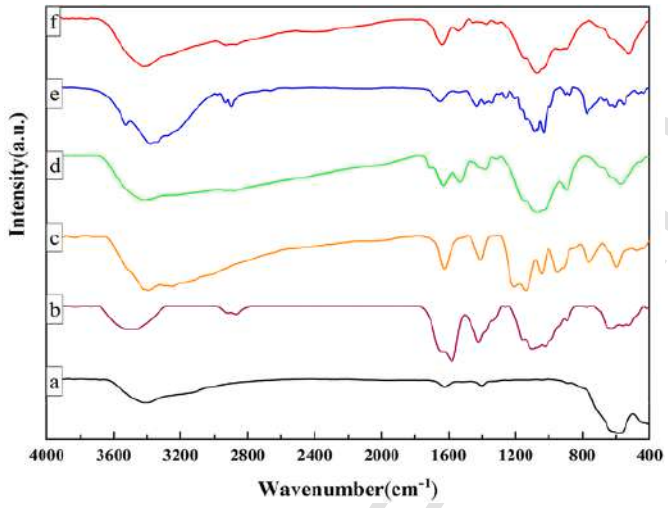

Fig. 4. FTIR spectra of Fe_3O_4 (a), Cs (b), MoS_2(c), Fe3O4/Cs/MoS_2 (d), Lac (e), Fe_3O_4/Cs/MoS_2/La (f) NPs.

assigned to the O–H, -CH2, bending vibrations of C═O and N–H, C–N, C–O, and C–*O*–C, respectively (Alizadeh Sani et al., 2022; Sani et al., 2023). Distinctive frequencies corresponding to the vibrations of Mo–O and Mo–S were detected and recorded to be situated at 599 cm^{-1} and 480 cm^{-1}, respectively (Cao et al., 2019). Additionally, the peak at 3382 cm^{-1} is related to the adsorbed H_2O. It is noteworthy that these results have noteworthy implications for the study of MoS_2 and its properties. Similarly, IR peaks of Fe_3O_4 nanoparticles were observed at 3402, 1623, 1400, 579, and 440 cm^{-1}. The emergence of peaks at 2931 cm^{-1} (CH_2) and 1715 cm^{-1} (C═O stretching) and the lack of an S–H group can be explained by the coupling of mercaptoacetic acid on MoS_2 in the context of Fe_3O_4/Cs/MoS_2/Lac (Qiu et al., 2021). The presence of the stretching vibrations of amide I at 1631 cm^{-1} (C–O and N–H) and the bending vibrations of amide II at 1522 cm^{-1} (N–H) in the IR spectra analysis of Cs and enzyme, suggests the formation of amide bonds (–NH–CO-) between Cs and mercaptoacetic acid on MoS_2, and the efficacious fabrication of Fe_3O_4/Cs/MoS_2 NPs loaded with Lac. The analysis conducted using FTIR spectroscopy provides conclusive evidence indicating that magnetic particles underwent the process of modification via the use of Cs and an enzyme (Silveira et al., 2020).

3.1.6. Particle size analysis

The particle size of the composite ingredients was determined using a particle size analyzer (PSA), as shown in Fig. 5. The results indicate a particle size range of 400–450 nm with a polydispersity index (PDI) of 0.15–0.2, suggesting good dispersion in the solution. This observation indicates that the surface modification did not affect the charge distribution of the nanoparticles, which is consistent with previous findings. This successful surface modification achieved the desired functionalization without compromising the inherent properties of the nanoparticles. The enhanced dispersion stability of the carrier is crucial for efficient enzyme immobilization, leading to improved catalytic performance and a longer lifespan for the immobilized enzymes. These factors contribute to a more cost-effective and sustainable application of the enzymes (Qiu et al., 2021; Khiavi et al., 2020; Kim et al., 2018; Cao et al., 2019; Geioushy et al., 2019b; Silveira et al., 2020).

3.1.7. VSM analysis

VSM measurements of the hysteresis curves revealed the magnetic properties of Fe_3O_4/MoS_2/Cs/Lac NPs, confirming superparamagnetic behavior with zero coercivity and remanence (Fig. 6). Fe_3O_4 NPs exhibited significant magnetization, measuring approximately 50 emu/g. This reduction in magnetization to 20 emu/g from 50 emu/g in Fe_3O_4 NPs is likely due to the presence of additional materials within the nanocomposites, which could influence the magnetic properties of the Fe_3O_4 NPs (Kadam et al., 2020; Ran et al., 2019). Furthermore, these nanocomposites exhibited easy separation from aqueous solutions. This

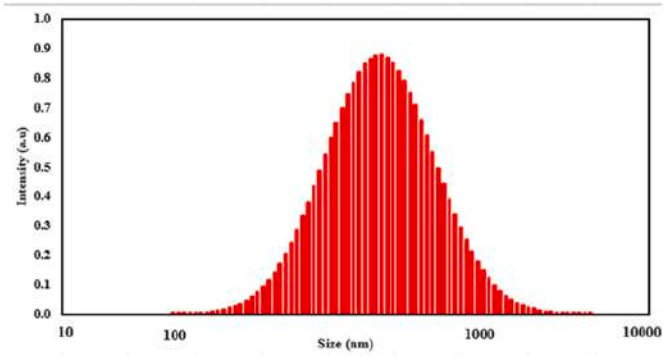

Fig. 5. Particle size of Fe_3O_4/Cs/MoS_2/Lac NPs.

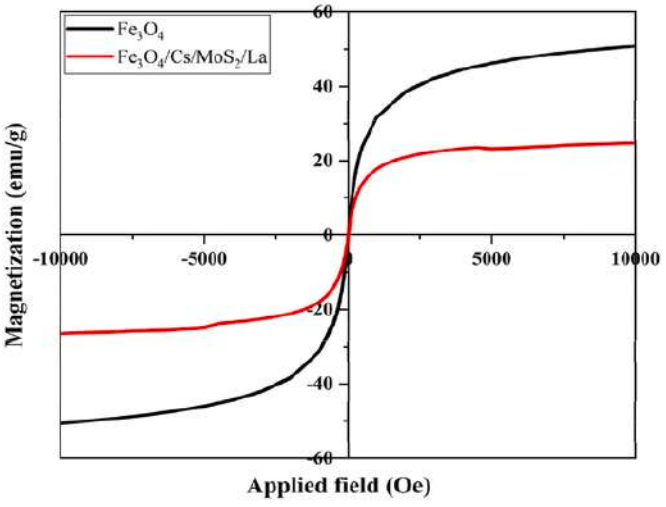

Fig. 6. Magnetic hysteresis loop of Fe_3O_4, and Fe_3O_4/MoS_2/Cs-Lac NPs.

unique combination of superparamagnetism and easy separation makes Fe_3O_4/MoS_2/Cs/Lac NPs promising materials for various industrial applications, such as magnetic separation, catalysis, and drug delivery within the field of materials science.

3.2. Laccase immobilization efficiency

Fe_3O_4/Cs/MoS_2 NPs were successfully employed for laccase immobilization, achieving a high immobilization efficiency with 95.8% activity recovery and a loading capacity of 2 mg/ml laccase. This immobilization strategy resulted in enhanced enzyme loading and activity, as shown in Table 1. Increasing the laccase concentration from 0.5 to 2 mg/ml led to a significant increase in IM-laccase activity from 48.6% to 96.8%. This improvement is attributed to the strong interaction between laccase and the carrier, as well as the favorable microenvironment provided by the ionic liquid structure, which facilitates enzyme binding to the substrate.

Previous research by Sadeghzadeh et al. (Sadeghzadeh et al., 2020; Zappi et al., 2018) demonstrated the successful immobilization of cross-linked laccase aggregates onto magnetic nanoparticles for bisphenol A removal. However, their approach resulted in a lower retention of bare laccase activity (27%), achieving an elimination efficiency of 87%.

The immobilization technology enables the reuse of laccase, reducing economic costs and promoting its practical application in various industries. This study found that immobilizing laccase onto the nanocomposite resulted in the highest level of AFM_1 reduction (68.5%) after 1 h. These findings demonstrate the potential for utilizing IM-Laccase as an efficient sorbent for AFM_1 removal.

3.3. MTT assay

The MTT assay was applied to measure the cell viability of L929 cells after 48 h of exposure to different concentrations (0.0625–160 ppm) of MoS_2 or Fe_3O_4/MoS_2/Cs NPs or Fe_3O_4/MoS_2/Cs/Lac NPs. The MTT results demonstrated that L929 cell viability was reduced in the presence of MoS_2 or Fe_3O_4/MoS_2/Cs NPs or Fe_3O_4/MoS_2/Cs/Lac NPs when compared with untreated control. The significant reduction in cell viability in the presence of MoS_2 started from a concentration of 20 ppm (% cell viability: 85.75 ± 5.48; $P < 0.05$) and reached to maximum in the 160 ppm (% cell viability: 57.70 ± 12.89; $P < 0.001$). The results showed that treatment with 20 (% cell viability: 76.64 ± 7.75; $P < 0.01$) to 160 ppm (% cell viability: 58.48 ± 3.9; $P < 0.001$) of Fe_3O_4/MoS_2/Cs nanoparticles causes a severe reduction in the percentage of L929 cell viability. The reduction of cell viability in a concentration of 10 ppm of Fe_3O_4/MoS_2/Cs (% cell viability: 89.12 ± 5.8; $P < 0.05$) was higher than MoS_2 (% cell viability: 93.69 ± 0.87). The cell viability of L929 normal cells in presence of 10, 20, 40, 80 and 160 ppm of Fe_3O_4/MoS_2/Cs/Lac NPs was 92.64 ± 2.5; ($P < 0.064$), 83.65 ± 1.6; ($P < 0.01$), 69.27 ± 6.04; ($P < 0.001$), 67.73 ± 0.08; ($P < 0.001$), and 57.93 ± 3.9; ($P < 0.001$). The reduction of cell viability in response to Fe_3O_4/MoS_2/Cs/Lac NPs was significant from a concentration of 20 ppm relative to the untreated control. Fe_3O_4/MoS_2/Cs/Lac NPs at concentrations ranging from 0.625 to 10 g/mL for 48 h did not affect cell viability. These findings demonstrated that Fe_3O_4/MoS_2/Cs/Lac NPs had no significant cytotoxic activity at concentrations less than 20 ppm; nonetheless, the cytotoxic effect of these rises with increasing concentration (Fig. 6).

Table 1
Immobilization efficiency Fe_3O_4/MoS_2/Cs-Lac NPs.

Laccase concentration (mg/ml)	Activity recovery (%)
0.5	48.6
1	67.1
1.5	81.6
2	96.8

The L929 cell viability in the response to MoS_2 or MoS_2/Fe/Cs NPs or Fe_3O_4/MoS_2/Cs/Lac NPs treatments. The cells were treated with different concentrations (0.0625–160 ppm) of the mentioned treatments for 48 h, and the percentage of cell viability was determined in compression with non-treated control. All values are shown as the mean ± SD of three individual experiments performed in triplicate and presented as the mean. *$p < 0.05$ **$p < 0.01$ and ***$p < 0.0001$ vs non-treated cells.

3.4. Effect of the sorbent type

The ability of the laccase, MoS_2 NPs, Fe_3O_4/Cs/MoS_2 NPs, and $Fe_3O_4/Cs/MoS_2$/Lac NPs to remove AFM_1 was compared using the removal percentage (R%). Each sorbent (40 mg) was individually added to 2 ml milk into microtubes containing AFM_1 with a concentration of 5 mg/l, followed by shaking for 40 min at 150 rpm. the removal percentage (R%) was calculated using the following equation:

$$R\% = \frac{C_i - C_f}{C_i} * 100$$

Where C_i and C_f are the spiked concentration of AFM_1 and the final concentration of AFM_1 in the milk sample after removing process. The results are presented in Table 2, indicating that the highest R% was obtained using $Fe_3O_4/Cs/MoS_2$/Lac NPs as a sorbent. Besides, MoS_2 NPs have the lowest R% which is due to the lowest interaction between MoS_2 NPs and AFM_1 through interaction between sulfur atoms in MoS_2 NPs and AFM_1 functional groups containing oxygen. A better R% was obtained using laccase as a sorbent because of hydrogen bonding between carboxyl and amine groups in laccase with AFM_1 functional groups containing oxygen atoms. A significant increase in R% was observed using Fe_3O_4/Cs/MoS_2 NPs compared to laccase as a sorbent that is due to the increase of the surface area of the sorbent using nanoparticle and hydrogen bonding between amine groups of chitosan with AFM_1 functional groups containing oxygen atoms. Finally, the synergistic effects of chitosan and laccase on the sorbent surface lead to the highest R% toward AFM_1.

3.5. Removal of AFM_1

The AFM_1 removal through different samples was investigated after three different contact times (20, 40, and 60 min) (Fig. 7). As depicted in this Figure, all the synthesized sorbents significantly removed AFM_1 from milk samples in the removal percentage ranges of 20%–70%. In general, increasing the contact time meaningfully increased the absorption of AFM_1 on all sorbents. The order of effect of different sorbents to remove AFM_1 was found as follows: $Fe_3O_4/Cs/MoS_2$/Lac NPs > Fe_3O_4/Cs/MoS_2 NPs > bare laccase. According to these results, the highest R% of AFM_1 (68.5%) was achieved using the immobilization of laccase enzyme into Fe_3O_4/Cs/MoS_2 NPs as a sorbent at a contact time of 60 min. However, it can be seen that the potency of the free enzyme is lower compared to the enzyme immobilized on Fe_3O_4/Cs/MoS_2 NPs. These outcomes are in line with the findings of the studies that reported that laccase enzyme immobilization on Fe_3O_4/Cs/MoS_2 NPs increases its stability and surface area to interact between functional groups of $Fe_3O_4/Cs/MoS_2$/Lac NPs with AFM_1,

Table 2
Effects of sorbent type on the removal of AFM_1.

Sorbent	R% ± SD[a]
MoS_2 NPs	22.36 ± 1.67
Laccase	26.87 ± 1.92
Fe_3O_4/Cs/MoS_2 NPs	47.42 ± 1.86
$Fe_3O_4/Cs/MoS_2$/Lac NPs	61.93 ± 1.84

[a] Removal percentage ± Standard devation

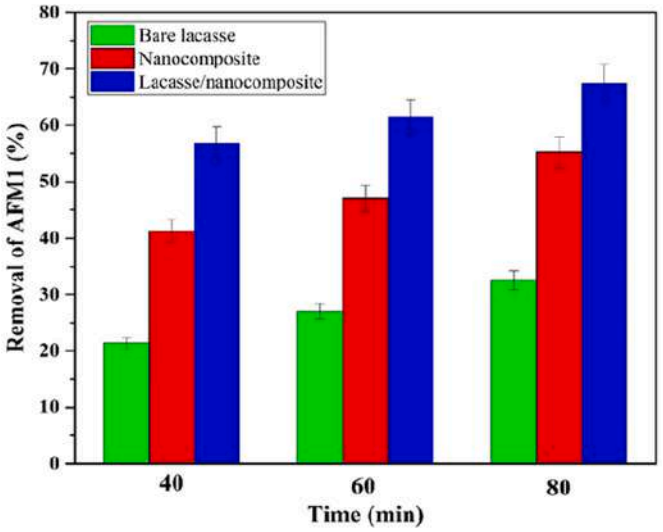

Fig. 7. The removal of AFM_1 in milk at different contact times with Bare laccase, synthesized nanocomposites, and immobilized laccase on nanocomposite samples.

leading to improvement in its performance as a sorbent (Kadam et al., 2020; Nadaroglu et al., 2019; Rostami et al., 2022). In other words, an increase in the removal percentages of AFM_1 using Fe_3O_4/Cs/MoS_2/Lac NPs is due to several properties of the sorbent. (i) Using Fe_3O_4/Cs/MoS_2 NPs as a sorbent component leads to an increase in the sorbent surface area, as a result, the R% of AFM_1 was enhanced. (ii) The presence of laccase enzyme immobilization on the sorbent can interact with AFM_1 through hydrogen bonding between carboxyl or amine groups of laccase enzyme and AFM_1 functional groups containing oxygen (ester or ether). (iii) Chitosan nanoparticles have the ability to chelate different compounds due to having amine functional groups (Ramadan et al., 2020). Therefore, chitosan nanoparticles can significantly interact with AFM_1 by the formation of hydrogen bonds between the functional group of chitosan and AFM_1. Other researchers have also stated similar findings (Abdelnaby et al., 2021; Hemmati et al., 2022).

4. Adsorption mechanism

Laccase is an enzyme that can degrade various pollutants. When immobilized on a nanocomposite, it retains its ability to interact with AFM_1, primarily through hydrogen bonding and electrostatic interactions (Fig. 8). The enzyme contains functional groups such as carboxyl (——COOH) and amino groups(——NH_2), which can form bonds with AFM_1 molecules. MoS_2 is used for its high surface area and ability to form a stable support structure. It can engage in π-π interactions with the aromatic rings of AFM_1, facilitating the adsorption process (Datta et al., 2021).

MoS_2 also provides a large surface area for the adsorption of AFM_1 (Geioushy et al., 2019b). Chitosan is a biopolymer with numerous amino groups that can interact with AFM_1 through hydrogen bonding and electrostatic interactions. The presence of these functional groups enhances the adsorption capacity of the nanocomposite (Liang et al., 2019). The magnetic core (Fe_3O_4) allows for the easy separation of the nanocomposite from the solution after adsorption. This magnetic property is crucial for practical applications, where the nanocomposite can be quickly removed from the contaminated sample. Both chitosan and laccase have functional groups that can form hydrogen bonds with AFM_1. Specifically, the hydroxyl(——OH), amino(——NH_2), and carboxyl (——COOH) groups in chitosan and laccase interact with the oxygen-containing functional groups in AFM_1 (such as the lactone ring and methoxy groups). Chitosan, being positively charged under acidic conditions, can interact with negatively charged regions of AFM_1. This interaction enhances the binding of AFM_1 to the nanocomposite, particularly in environments where AFM_1 is partially ionized. MoS_2, a layered material with delocalized π-electrons, can interact with the aromatic rings of AFM_1 through π-π stacking (Ran et al., 2019). This non-covalent interaction adds another layer of adsorption, stabilizing the AFM_1 mole-

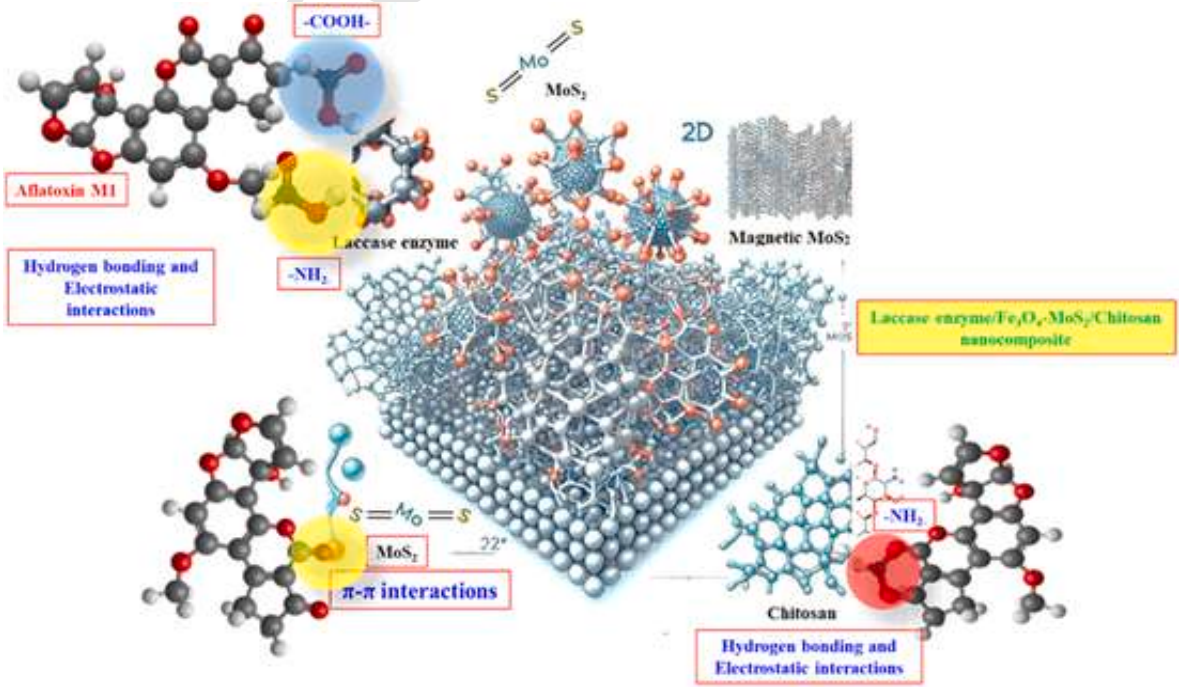

Fig. 8. Possible mechanism of AFM_1 adsorption on Fe_3O_4/Cs/MoS_2/Lac NPs.

cules on the nanocomposite surface. These functional groups contribute to the overall adsorption process by providing multiple avenues for interactions, leading to strong binding and efficient adsorption of AFM_1 onto the Fe_3O_4/Cs/MoS_2/Lac NPs (Sirajudheen et al., 2024).

4.1. Composition of AFM_1 in milk

According to the results, the proposed adsorbent has a high capability for interaction and efficient adsorption of AFM_1 in milk samples. The combination of these interactions—hydrogen bonding, electrostatic forces, π-π stacking, and physical adsorption—creates a synergistic effect, leading to a high adsorption efficiency of the nanocomposite (Nicolle et al., 2021). Each component enhances the overall performance, making the composite more effective than any single material alone. When the magnetic Laccase/MoS_2/Chitosan nanocomposite is introduced into an AFM_1-contaminated solution (e.g., milk), the following steps occur (Nicolle et al., 2021).

1) AFM_1 molecules diffuse towards the surface of the nanocomposite due to concentration gradients.
2) AFM_1 initially binds to the surface of the nanocomposite through hydrogen bonding and electrostatic interactions with chitosan and laccase.
3) The AFM_1 molecules further stabilize on the nanocomposite surface through π-π stacking with MoS_2 and physical adsorption in the pores and on the surface of the nanocomposite.
4) After sufficient contact time, the nanocomposite, now loaded with AFM_1, can be easily separated from the solution using an external magnetic field.

The highest removal efficiency observed in the study was 68.5% after 60 min of contact time, indicating that the nanocomposite is highly effective in adsorbing AFM_1 from milk samples. This efficiency is attributed to the combined effects of high surface area, multiple interaction mechanisms, and the stable immobilization of laccase on the nanocomposite.

5. Conclusions

The Fe_3O_4/Cs/MoS_2 NPs prepared in this study showed great potential as a laccase carrier for the efficient removal of AFM_1 from milk samples. The successful immobilization of laccase onto the nanoparticles was confirmed through various analyses, and the highest removal efficiency of 68.5% was achieved in just 1 h. Under optimum conditions, a loading laccase amount of 2 mg/ml on Fe_3O_4/Cs/MoS_2 NPs with an immobilization efficiency of 96.8% was obtained. The MTT assay indicated that Fe_3O_4/MoS_2/Cs/Lac NPs had no significant cytotoxic activity at concentrations less than 20 ppm. These results suggest that Fe_3O_4/MoS_2/Cs/Lac NPs could be a promising solution for environmental protection applications, offering improved performance in AFM_1 removal compared to bare laccase enzyme, MoS_2 NPs, and Fe_3O_4/MoS_2/Cs. This study highlights the potential of these composite nanoparticles as effective enzyme carriers for environmental remediation.

CRediT authorship contribution statement

Alieh Rezagholizade-shirvan: Writing – review & editing, Writing – original draft, Validation, Methodology, Investigation.

Declaration of competing interest

The authors have declared no conflict of interest.

Acknowledgments

The authors gratefully acknowledge the financial and technical support of the Neyshabur University of Medical Sciences, Neyshabur, Iran (Grant number: 1400-01-267).

Data availability

The data that has been used is confidential.

References

Abdelnaby, A., Abdelaleem, N.M., Elshewy, E., Mansour, A.H., Ibrahim, S., 2021. The efficacy of clay bentonite, date pit, and chitosan nanoparticles in the detoxification of aflatoxin M1 and ochratoxin A from milk. Environ. Sci. Pollut. Control Ser. 1–13.
Abdi-Moghadam, Z., Mazaheri, Y., Rezagholizade-Shirvan, A., Mahmoudzadeh, M., Sarafraz, M., Mohtashami, M., Shokri, S., Ghasemi, A., Nickfar, F., Darroudi, M., 2023a. The significance of essential oils and their antifungal properties in the food industry: a systematic review. Heliyon e21386.
Abdi-Moghadam, Z., Darroudi, M., Mahmoudzadeh, M., Mohtashami, M., Jamal, A.M., Shamloo, E., Rezaei, Z., 2023b. Functional Yogurt, Enriched and Probiotic: A Focus on Human Health. Clinical Nutrition ESPEN.
Alameri, M.M., Kong, A.S.-Y., Aljaafari, M.N., Ali, H.A., Eid, K., Sallagi, M.A., Cheng, W.-H., Abushelaibi, A., Lim, S.-H.E., Loh, J.-Y., 2023. Aflatoxin contamination: an overview on health issues, detection and management strategies. Toxins 15, 246.
Alizadeh Sani, M., Khezerlou, A., Tavassoli, M., Mohammadi, K., Hassani, S., Ehsani, A., McClements, D.J., 2022. Bionanocomposite active packaging material based on soy protein Isolate/Persian Gum/Silver nanoparticles; fabrication and characteristics. Colloids and Interfaces 6, 57.
Alvarado-Ramírez, L., Rostro-Alanis, M., Rodríguez-Rodríguez, J., Castillo-Zacarías, C., Sosa-Hernández, J.E., Barceló, D., Iqbal, H.M., Parra-Saldívar, R., 2021. Exploring current tendencies in techniques and materials for immobilization of laccases–A review. Int. J. Biol. Macromol. 181, 683–696.
Aoyanagi, M.M.d.C.C., Budiño, F.E.L., Raj, J., Vasiljević, M., Ali, S., Ramalho, L.N.Z., Ramalho, F.S., Corassin, C.H., Ghantous, G.F., Oliveira, C.A.F.d., 2023. Efficacy of two commercially available adsorbents to reduce the combined toxic effects of dietary Aflatoxins, Fumonisins, and Zearalenone and their residues in the tissues of weaned pigs. Toxins 15, 629.
Atabati, H., Kassiri, H., Shamloo, E., Akbari, M., Atamaleki, A., Sahlabadi, F., Linh, N.T.T., Rostami, A., Fakhri, Y., Khaneghah, A.M., 2020. The association between the lack of safe drinking water and sanitation facilities with intestinal Entamoeba spp infection risk: a systematic review and meta-analysis. PLoS One 15, e0237102.
Azari, A., Kamani, H., Sarkhosh, M., Vatankhah, N., Yousefi, M., Mahmoudi-Moghaddam, H., Razavinasab, S.A., Masoudi, M.R., Sadeghi, R., Sharifi, N., 2024. Nectarine core-derived magnetite biochar for ultrasound-assisted preconcentration of polycyclic aromatic hydrocarbons (PAHs) in tomato paste: a cost-effective and sustainable approach. Food Chem. X 24, 101810.
Cao, W., Yue, L., Wang, Z., 2019. High antibacterial activity of chitosan–molybdenum disulfide nanocomposite. Carbohydrate polymers 215, 226–234.
Datta, S., Veena, R., Samuel, M.S., Selvarajan, E., 2021. Immobilization of laccases and applications for the detection and remediation of pollutants: a review. Environ. Chem. Lett. 19, 521–538.
Deng, J., Zhao, L., Zhang, N.-Y., Karrow, N.A., Krumm, C.S., Qi, D.-S., Sun, L.-H., 2018. Aflatoxin B1 metabolism: regulation by phase I and II metabolizing enzymes and chemoprotective agents. Mutation research/reviews in mutation research 778, 79–89.
Fallah, A.A., 2010. Aflatoxin M1 contamination in dairy products marketed in Iran during winter and summer. Food Control 21, 1478–1481.
Farhadi, L., Mohtashami, M., Saeidi, J., Azimi-nezhad, M., Taheri, G., Khojasteh-Taheri, R., Rezagholizade-Shirvan, A., Shamloo, E., Ghasemi, A., 2022. Green synthesis of chitosan-coated silver nanoparticle, characterization, antimicrobial activities, and cytotoxicity analysis in cancerous and normal cell lines. J. Inorg. Organomet. Polym. Mater. 32, 1637–1649.
Geioushy, R.A., El-Sheikh, S.M., Hegazy, I.M., Shawky, A., El-Sherbiny, S., Kandil, A.-H.T., 2019a. Insights into two-dimensional MoS2 sheets for enhanced CO2 photoreduction to C1 and C2 hydrocarbon products. Mater. Res. Bull. 118, 110499.
Geioushy, R., El-Sheikh, S., Hegazy, I., Shawky, A., El-Sherbiny, S., Kandil, A.-H.T., 2019b. Insights into two-dimensional MoS2 sheets for enhanced CO2 photoreduction to C1 and C2 hydrocarbon products. Mater. Res. Bull. 118, 110499.
Ghorbani, M., Chamsaz, M., Rounaghi, G.H., 2016. Ultrasound-assisted magnetic dispersive solid-phase microextraction: a novel approach for the rapid and efficient microextraction of naproxen and ibuprofen employing experimental design by high-performance liquid chromatography. J. Separ. Sci. 39, 1082–1089.
Ghorbani, M., Shams, A., Seyedin, O., Afshar Lahoori, N., 2017. Magnetic ethylene diamine-functionalized graphene oxide as novel sorbent for removal of lead and cadmium ions from wastewater samples. Environ. Sci. Pollut. Control Ser. 25, 5655–5667.
Ghorbani, M., Aghamohammadhassan, M., Chamsaz, M., Akhlaghi, H., Pedramrad, T., 2019. Dispersive solid phase microextraction. TrAC, Trends Anal. Chem. 118, 793–809.
Ghorbani, M., Seyedin, O., Aghamohammadhassan, M., 2020a. Adsorptive removal of lead (II) ion from water and wastewater media using carbon-based nanomaterials as unique sorbents: a review. J. Environ. Manag. 254, 109814.

Ghorbani, M., Aghamohammadhassan, M., Ghorbani, H., Zabihi, A., 2020b. Trends in sorbent development for dispersive micro-solid phase extraction. Microchem. J. 158, 105250.
Ghorbani, M., Keshavarzi, M., Pakseresht, M., Mohammadi, P., Shams, A., Mehraban, A., Ismailzadeh, A., 2023. Optimization and synthesis of a novel sorbent composite based on magnetic chitosan-amine-functionalized bimetallic MOF for the simultaneous dispersive solid-phase microextraction of four aflatoxins in real water, herbal distillate, and food samples. Anal. Bioanal. Chem. 415, 5681–5694.
Ghorbani, M., Saghafi, A., Pakseresht, M., Shams, A., Keshavarzi, M., Asghari, S., 2024. Crafting an innovative bimetallic MOF-on-MOF/TiO2 composite for effective removal of imatinib anticancer agent through adsorption and photodegradation. Separation and Purification Technology 126227.
Gordi, Z., Ghorbani, M., Ahmadian Khakhiyani, M., 2020. Adsorptive removal of enrofloxacin with magnetic functionalized graphene oxide@ Metal-organic frameworks employing D-optimal mixture design. Water Environ. Res. 92, 1935–1947.
Hamad, G.M., El-Makarem, H.S.A., Allam, M.G., El Okle, O.S., El-Toukhy, M.I., Mehany, T., El-Halmouch, Y., Abushaala, M.M., Saad, M.S., Korma, S.A., 2023. Evaluation of the adsorption efficacy of bentonite on aflatoxin M1 levels in contaminated milk. Toxins 15, 107.
Hemmati, F., Hosseini, H., Mirmoghtadaei, L., Mirzaei, E., Mofid, V., Mazloomi, S.M., Karimian-Khosroshahi, N., Mortazavian, A.M., Mousavi Khaneghah, A., 2022. Mitigation of aflatoxin M1 in milk by the magnetized Fe3O4 lactic acid bacteria cells: a response surface methodology (RSM) study. Int. J. Environ. Anal. Chem. 1–16.
Jahanmard, E., Keramat, J., Nasirpour, A., Emadi, R., 2021. Efficiency of calcined Aluminum-Magnesium layered double hydroxide for adsorption of aflatoxin M1 from solution and matrix of milk. J. Food Sci. 86, 5200–5212.
Kadam, A.A., Sharma, B., Shinde, S.K., Ghodake, G.S., Saratale, G.D., Saratale, R.G., Kim, D.-Y., Sung, J.-S., 2020. Thiolation of chitosan loaded over super-magnetic halloysite nanotubes for enhanced laccase immobilization. Nanomaterials 10, 2560.
Khiavi, N.M.N., Khiabani, M.S., Mokarram, R.R., Kafil, H.S., 2020. Reduction of aflatoxin M1 using mixture of Saccharomyces cerevisiae and Candida albicans cell walls immobilized on silica nanoparticles entrapped in alginate gel. J. Environ. Chem. Eng. 8, 103635.
Khosravi-Darani, K., Gomes da Cruz, A., Shamloo, E., Abdimoghaddam, Z., Mozafari, M., 2019. Green synthesis of metallic nanoparticles using algae and microalgae. Letters in Applied NanoBioScience 8, 666–670.
Kim, M., Jee, S.C., Sung, J.-S., Kadam, A.A., 2018. Anti-proliferative applications of laccase immobilized on super-magnetic chitosan-functionalized halloysite nanotubes. Int. J. Biol. Macromol. 118, 228–237.
Liang, X.X., Omer, A., Hu, Z.-h., Wang, Y.g., Yu, D., Ouyang, X.-k., 2019. Efficient adsorption of diclofenac sodium from aqueous solutions using magnetic amine-functionalized chitosan. Chemosphere 217, 270–278.
Liu, Y., Mao, H., Hu, C., Tron, T., Lin, J., Wang, J., Sun, B., 2020. Molecular docking studies and in vitro degradation of four aflatoxins (AFB1, AFB2, AFG1, and AFG2) by a recombinant laccase from Saccharomyces cerevisiae. Journal of food science 85, 1353–1360.
Meneely, J.P., Kolawole, O., Haughey, S.A., Miller, S.J., Krska, R., Elliott, C.T., 2023. The challenge of global aflatoxins legislation with a focus on peanuts and peanut products: a systematic review. Exposure and Health 15, 467–487.
Mimoune, N.A., Riba, A., Verheecke, C., Mathieu, F., Sabaou, N., 2016. Fungal contamination and mycotoxin production by Aspergillus spp. in nuts and sesame seeds. J. Microbiol. Biotechnol. Food Sci. 5, 301.
Min, L., Fink-Gremmels, J., Li, D., Tong, X., Tang, J., Nan, X., Yu, Z., Chen, W., Wang, G., 2021. An overview of aflatoxin B1 biotransformation and aflatoxin M1 secretion in lactating dairy cows. Animal Nutrition 7, 42–48.
Muaz, K., Riaz, M., Oliveira, C.A.F.d., Ismail, A., Akhtar, S., Nadeem, H., Waseem, S., Ahmed, Z., 2024. Aflatoxin M1 removal from milk using activated carbon and bentonite combined with lactic acid bacteria cells. Int. J. Dairy Technol. 77, 393–402.
Muthuvelu, K.S., Rajarathinam, R., Selvaraj, R.N., Rajendren, V.B., 2020. A novel method for improving laccase activity by immobilization onto copper ferrite nanoparticles for lignin degradation. Int. J. Biol. Macromol. 152, 1098–1107.
Nadaroglu, H., Mosber, G., Gungor, A.A., Adıguzel, G., Adiguzel, A., 2019. Biodegradation of some azo dyes from wastewater with laccase from Weissella viridescens LB37 immobilized on magnetic chitosan nanoparticles. Journal of Water Process Engineering 31, 100866.
Nazifi, M., Ramezani, A.M., Absalan, G., Ahmadi, R., 2021. Colorimetric determination of D-penicillamine based on the peroxidase mimetic activity of hierarchical hollow MoS2 nanotubes. Sensor. Actuator. B Chem. 332, 129459.
Nicolle, L., Journot, C.M., Gerber-Lemaire, S., 2021. Chitosan functionalization: covalent and non-covalent interactions and their characterization. Polymers 13, 4118.
Organization, W.H., Cancer, I.A.f.R.o., 1993. Some naturally occurring substances: food items and constituents, heterocyclic aromatic amines and mycotoxins. IARC (Int. Agency Res. Cancer) Monogr. Eval. Carcinog. Risk Chem. Hum. 56.
Othman, A., Dumitrescu, E., Andreescu, D., Andreescu, S., 2018. Nanoporous sorbents for the removal and recovery of phosphorus from eutrophic waters: sustainability challenges and solutions. ACS Sustain. Chem. Eng. 6, 12542–12561.
Pickova, D., Ostry, V., Toman, J., Malir, F., 2021. Aflatoxins: history, significant milestones, recent data on their toxicity and ways to mitigation. Toxins 13, 399.
Qiu, X., Wang, S., Miao, S., Suo, H., Xu, H., Hu, Y., 2021. Co-immobilization of laccase and ABTS onto amino-functionalized ionic liquid-modified magnetic chitosan nanoparticles for pollutants removal. J. Hazard Mater. 401, 123353.
Ramadan, M.M., Mohamed, M.A., Almoammar, H., Abd-Elsalam, K.A., 2020. Magnetic nanomaterials for purification, detection, and control of mycotoxins. In: Nanomycotoxicology. Elsevier, pp. 87–114.
Ran, F., Zou, Y., Xu, Y., Liu, X., Zhang, H., 2019. Fe3O4@ MoS2@ PEI-facilitated enzyme tethering for efficient removal of persistent organic pollutants in water. Chem. Eng. J. 375, 121947.
Rezagholizade-shirvan, A., Najafi, M.F., Behmadi, H., Masrournia, M., 2022. Preparation of nano-composites based on curcumin/chitosan-PVA-alginate to improve stability, antioxidant, antibacterial and anticancer activity of curcumin. Inorg. Chem. Commun. 145, 110022.
Rezagholizade-Shirvan, A., Kalantarmahdavi, M., Amiryousefi, M.R., 2023a. Evaluation of the effect of basil seed gum, tragacanth gum, pectin, and coating formulation with corn flour on oil absorption and sensory properties of watermelon rind chips. Heliyon 9, e16976.
Rezagholizade-shirvan, A., Masrournia, M., Fathi Najafi, M., Behmadi, H., 2023b. Synthesis and characterization of nanoparticles based on chitosan-biopolymers systems as nanocarrier agents for curcumin: study on pharmaceutical and environmental applications. Polym. Bull. 80, 1495–1517.
Rezagholizade-Shirvan, A., Mohammadi, M., Mazaheri, Y., Fallahizadeh, S., Ghorbani, H., Shokri, S., Shariatifar, N., Darroudi, M., Shamloo, E., 2024. Employing a magnetic chitosan/molybdenum disulfide nanocomposite for efficiently removing polycyclic aromatic hydrocarbons from milk samples. Sci. Rep. 14,15054.
Rostami, A., Abdelrasoul, A., Shokri, Z., Shirvandi, Z., 2022. Applications and mechanisms of free and immobilized laccase in detoxification of phenolic compounds—a review. Kor. J. Chem. Eng. 39, 821–832.
Rubio-Govea, R., Hickey, D.P., Garcia-Morales, R., Rodriguez-Delgado, M., Dominguez-Rovira, M.A., Minteer, S.D., Ornelas-Soto, N., Garcia-Garcia, A., 2020. MoS2 nanostructured materials for electrode modification in the development of a laccase based amperometric biosensor for non-invasive dopamine detection. Microchem. J. 155, 104792.
Sadeghzadeh, S., Nejad, Z.G., Ghasemi, S., Khafaji, M., Borghei, S.M., 2020. Removal of bisphenol A in aqueous solution using magnetic cross-linked laccase aggregates from Trametes hirsuta. Bioresour. Technol. 306, 123169.
Sani, M.A., Dabbagh-Moghaddam, A., Jahed-Khaniki, G., Ehsani, A., Sharifan, A., Khezerlou, A., Tavassoli, M., Maleki, M., 2023. Biopolymers-based multifunctional nanocomposite active packaging material loaded with zinc oxide nanoparticles, quercetin and natamycin; development and characterization. J. Food Meas. Char. 1–17.
Schrenk, D., Bignami, M., Bodin, L., Chipman, J.K., delMazo, J., Grasl-Kraupp, B., Hogstrand, C., Hoogenboom, L., Leblanc, J.C., EFSA Panel on Contaminants in the Food Chain, 2020. Risk assessment of aflatoxins in food. EFSA J. 18, e06040.
Seid, A., Mama, A., 2019. Aflatoxicosis and occurrence of aflatoxin M1 (AFM1) in milk and dairy products: a review. Austin Journal of Veterinary Science & Animal Husbandry 1, 1–12.
Shamloo, E., Jalali, M., 2015. Prevalence of Listeria species in raw milk and traditional dairy products in Isfahan, Iran. Int. J. Environ. Health Eng. 4, 1.
Shamloo, E., Jalali, M., Mirlohi, M., Abdi Moghadam, Z., Reza Maracy, M., Yaran, M., 2012. Prevalence of Listeria Species in Raw Milk in Isfahan, Iran, vol. 30. Journal of Isfahan Medical School.
Shamloo, E., Nickfar, F., Mahmoudzadeh, M., Sarafraz, M., Salari, A., Darroudi, M., Abdi-Moghadam, Z., Amiryosefi, M.R., Rezagholizade-Shirvan, A., Rezaei, Z., 2023. Investigation of heavy metal release from variety cookware into food during cooking process. Int. J. Environ. Anal. Chem. 1–17.
Shokri, S., Shariatifar, N., Molaee-Aghaee, E., Khaniki, G.J., Sadighara, P., Faramarzi, M.A., Mohammadi, M., Rezagholizade-Shirvan, A., 2023. Synthesis and characterization of a novel magnetic chitosan–nickel ferrite nanocomposite for antibacterial and antioxidant properties. Sci. Rep. 13, 15777.
Shokri, S., Shariatifar, N., Molaee-Aghaee, E., Jahed Khaniki, G., Sadighara, P., Faramarzi, M.A., 2024. Modeling sunset yellow removal from fruit juice samples by a novel chitosan-nickel ferrite nano sorbent. Sci. Rep. 14, 208.
Shokri-Jokari, S., Mirlohi, M., Mosharraf, L., 2016. Flour and bread aflatoxin contamination and risk assessment of aflatoxin intake through bread consumption in Iran. Journal of Isfahan Medical School 33, 2420–2428.
Silveira, T.R., Ebling, C.D., Dal Magro, L., Rodrigues, R.C., Schneider, W.D.H., Camassola, M., de Menezes, E.W., Meneguzzi, Á., Klein, M.P., 2020. An efficient decolorization of methyl orange dye by laccase from Marasmiellus palmivorus immobilized on chitosan-coated magnetic particles. Biocatal. Agric. Biotechnol. 30, 101859.
Sirajudheen, P., Vigneshwaran, S., Thomas, N., Selvaraj, M., Venkatesan, K., Park, C.M., 2024. Fabrication of MoS2 restrained magnetic chitosan polysaccharide composite for the photocatalytic degradation of organic dyes. Carbohydrate Polymers 335, 122071.
Yadav, D., Ranjan, B., Mchunu, N., Le Roes-Hill, M., Kudanga, T., 2021. Enzymatic treatment of phenolic pollutants by a small laccase immobilized on APTES-functionalised magnetic nanoparticles. 3 Biotech 11, 1–12.
Yang, J., Wang, T., Lin, G., Li, M., Zhu, R., Yiannikouris, A., Zhang, Y., Mai, K., 2020. The assessment of diet contaminated with aflatoxin B1 in juvenile turbot (Scophthalmus maximus) and the evaluation of the efficacy of mitigation of a yeast cell wall extract. Toxins 12, 597.
Yousefi, M., Farzadkia, M., Mahvi, A.H., Kermani, M., Gholami, M., Esrafili, A., 2024. Photocatalytic degradation of ciprofloxacin using a novel carbohydrate-based nanocomposite from aqueous solutions. Chemosphere 349, 140972.
Zappi, D., Masci, G., Sadun, C., Tortolini, C., Antonelli, M.L., Bollella, P., 2018. Evaluation of new cholinium-amino acids based room temperature ionic liquids (RTILs) as immobilization matrix for electrochemical biosensor development: proof-of-concept with Trametes Versicolor laccase. Microchem. J. 141, 346–352.
Zhang, Y., Li, X., Li, D., Wei, Q., 2020a. A laccase based biosensor on AuNPs-MoS2 modified glassy carbon electrode for catechol detection. Colloids Surf. B Biointerfaces 186, 110683.
Zhang, K., Yang, W., Liu, Y., Zhang, K., Chen, Y., Yin, X., 2020b. Laccase immobilized on chitosan-coated Fe3O4 nanoparticles as reusable biocatalyst for degradation of chlorophenol. J. Mol. Struct. 1220, 128769.